Band-gap states in unfilled mesoporous nc-TiO2: measurement protocol for electrical characterization

UNIVERSITÀ DEGLI STUDI DI TORINO

A. Cultrera, L. Boarino, G. Amato, C. Lamberti,

"Band gap states in unfilled mesoporous nc-TiO_2: measurement protocol for electrical characterization"

J. Phys. D-Appl. Phys., **47** (2014) Art. n. 015102.

DOI: 10.1088/0022-3727/47/1/015102

Band gap states in unfilled mesoporous nc-TiO_2: measurement protocol for electrical characterization

A Cultrera[1], L Boarino[2], G Amato[2], and C Lamberti[1]

[1] Department of Chemistry, NIS Centre of Excellence and INSTM Reference Center, Via Quarello 11, Università di Torino, 10135 Torino, Italy

[2] Electromagnetic Division, I.N.Ri.M., Strada delle Cacce 91, 10135 Torino, Italy

E-mail: alessandro.cultrera@unito.it

Abstract. Characterization of intrinsic electrical properties of large surface area materials like mesoporous nanocrystalline (nc-TiO_2), requires to avoid sensor-like response to external agents. Both an appropriate sample configuration and a suitable measurement protocol are mandatory. In this work both stack and planar contacts configuration were studied, the latter giving evidence to be potentially useful for space charge limited (SCL) current investigations in order to study the band-gap states (BGS) properties in nc-TiO_2. Moreover in absence of a suitable measurement protocol, standard dye sensitized solar cells (DSSC) electrode films show apparent SCL current behavior, as consequence of surface electrical transport contribution due to physisorbed water on the hydroxylated metal oxide large surface area. This feature recalls the typical results of electrolyte filled systems, in which an exponential distribution of trap states is reported, and it is not expected to be the intrinsic feature of nc-TiO_2 trap states distribution. In absence of adsorbates, no deviation from ohmic regime is observed in standard electrodes, while in planar configuration samples the SCL regime is accessible and shows a different BGS signature. The nature of the electrical contacts, ohmic in the present situation, is also discussed.

PACS numbers: 72.20.-i, 51.50.+v, 88.40.hj

1. Introduction

Mesoporous nanocrystalline TiO_2 films represent one of the basic components in Dye Sensitized Solar Cells [1, 2], and are extensively employed also in sensors [3, 4] and heterogeneous photocatalysis [5, 6]. The high impact of the these applications, the need of materials related to the development of renewable energy sources like the solar one, and the low cost of raw TiO_2, makes titania one of the most investigated oxides in the last decade [7]. In this context, a thorough electrical characterization of the TiO_2 based materials is a key point of this research line. Several techniques allow for the synthesis of highly crystalline titania powders for mesoporous nc-TiO_2 films [8]. The basic arrangement of titania nanopowders, when deposed in form of untemplated thin films, is the large specific surface area of the network of randomly interconnected nano-crystals [9]. On a similar ground, templated nanostructures exist in which TiO_2 structures are ordered at a certain degree [10]. Literature on electrical characterization of a broad range of systems and devices based on filled porous titania is very rich. As an example, sophisticated techniques, like impedance spectroscopy have been applied to DSSC to investigate the electrical properties of their components as separate systems by means of equivalent circuit models [11], and detailed simulations like TiberCAD allow to model the electrical properties of complete cells (or their separated components) [12].

It is not surprising that dry TiO_2 systems are less investigated due to the challenging task of performing steady state electrical measurements on unfilled porous structures [13, 14, 15, 16]. The improvement of the experimental characterization of unfilled porous systems, as a tool to get rid of some complexities due to electrolytes (liquid or solid) and dyes and for yielding experimental results about mesoporous titania structures solely, is of great importance and allows for direct comparison with other experimental techniques. The first step in this direction is to adopt a suitable measurement protocol. The main issue to be resolved is related to the apparent behavior induced by adsorbed water. This, commonly called as the Grotthuss effect, is the basic working principle of metal oxide based humidity sensors, but must be avoided if interested in probing the intrinsic properties of the material [17].

To better figure out the strong role of adsorbates in TiO_2 based systems, note that some authors work, both on theoretical and experimental grounds, on composite materials in which adsorbed CNTs or Fullerene generate localized states within TiO_2 band-gap. These are investigated in order to be exploited to achieve enhancements in photocatalytic or photovoltaic performances [18, 19, 20, 21].

Moreover, depending on the choice of the sample configuration it is possible to yield more or less information about the intrinsic properties of the material. In fact, the high resistivity of the material (of the order of $G\Omega\ m$), poses a limit to the achievable excess carrier concentration, mandatory to induce a deviation from the ohmic regime, useful to obtain information about band gap states distribution. In fact the more probed volume between the electrodes the larger is the overall series resistance of the network. This would require higher voltage to drive the conduction over the ohmic regime.

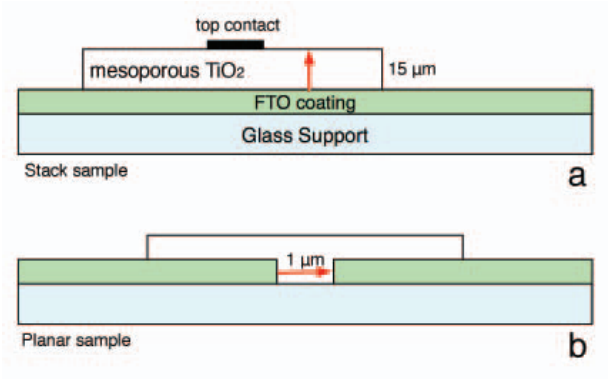

Figure 1. Stack and planar sample configurations. Arrows are indicative of electric field distribution under bias.

As a first approach, we studied commercial DSSC electrodes as a standard model to define our measurement protocol. Then we employed a more sophisticated sample configuration (planar instead of stack) in which it is possible to tailor and control the contact geometry so to inject higher values for current density through the sample. This way, intrinsic SCL transport regimes are reached allowing for for band-gap states investigations [22, 23, 24].

2. Experimental

2.1. Samples preparation

For measurements in stack contact geometry, commercial mesoporous nc-TiO_2 films (Dyesol) have been employed. The choice of using commercial samples where available, was dictated by the need of avoiding as much as possible reproducibility issues due to sample synthesis. These samples (figure 1-a) consist of FTO glass plates (SnO_2:F, 15 ohm/sq) on which 8 mm x 11 mm porous titania films have been screen-printed, with no intermediate TiO_2 compact blocking layer. The colloidal precursor is composed of 20 nm crystals including a certain amount of scattering particles with diameter around 400 nm. The thickness of the nc-TiO_2, as confirmed by surface profiling, is about 15 µm. The samples were used as received with no additional treatments others than rinse with ethanol before making top electrical contacts.

For the planar geometry configuration (figure 1-b), FTO glass supports of the same type as before have been used. FTO was scribed in longitudinal direction by means of a diamond scriber to obtain 3 mm large conductive strips. Focused Ion Beam techniques were exploited to etch the FTO in transversal direction in order to obtain μm-scale channels, which interrupted the conductive strip. Then P25 based colloid was deposited and subsequently sintered at 450 °C for 30 minutes. Titania colloid in this case was hand made. This way, the electric contacts, both of the same type, were adjoined at 1 µm distance. The thickness of the FTO is around 300 nm with a sharp step profile. The etched trenches were deeper than the FTO to avoid any leakage current components

through possible residual FTO. In this case the probed material volume is much smaller (about $10^{-6}\,\mathrm{mm}^3$ instead of $1\,\mathrm{mm}^3$).

Even though the nanocrystalline titania present in the two different types of sample was not the same (though analogue), and both were even multidispersed, it does not represent a concerning for our discussion. In fact in this work we present a protocol to face measurement issues that are common to nanostructured TiO_2 in general.

In stacked geometry, the top contacts onto titania film have been realized by painting graphite conductive cement (Leit-C carbon adhesive) and colloidal silver paste (Pelco conductive silver 187) using a plastic mask as stencil template. Silver colloidal paste was also used to make contact between the top graphite electrodes and small gauge gold wires. These pastes are both composed by micrometer gauge flat flakes so the diffusion of electrode material within the porous matrix is reasonably prevented. The main solvents were xylene and acetone respectively. Producers also declare small quantities of 4-(trifluoromethyl)-chlorobenzene and traces of ethyl benzene in colloidal silver paste, and 2-methoxy-1-methylethyl-acetate and ethyl-acetate for the graphite cement. Conductance test with air dryed and vacuum dryed top contacts, showed that if any, the effect of residual contamination of these solvents did not affect our results. In both cases, the connection of the samples to the experimental setup was realized with small gauge gold wires (AWG 36) bonded on one side to the samples and on the other to terminal pins on a sample-holder base by means of colloidal silver paste. The stacked samples were connected to the source-meter by grounding the bottom contact. So, in direct polarization electrons were injected through the bottom contact (FTO/TiO_2). Planar samples were symmetric.

2.2. Measurement chamber

The measurements were performed into a Janis ST-100 cryostat to minimize and tightly control the ambient conditions. The chamber was evacuated by means of a standard dry scroll/turbo pumps configuration. The sample temperature was kept constant (300 K) by a LakeShore 331 temperature controller. The electrical measurements, always in dark conditions, were performer by means of a Keithley 2410 source-meter in two-wire configuration.

2.3. Raman spectroscopy

Raman spectra were collected by use of a Madatech *i*-Raman spectrometer in backscattering geometry. A 532 nm laser was used as the excitation source. All spectra were collected in air at room temperature.

2.4. Surface profiling

Surface profiling of TiO_2 films and FTO supports have been performed by means of a Tencor P-10 stylus profiler.

3. Results and discussion

After the samples preparation and loading into the chamber, they were left to equilibrate under measurement at 0V bias to drain residual trapped charge once reached the desired ambient conditions. We observed persistent photoconductivity that introduced apparent features to dark current measurements even after hours for samples stored under ambient light. This is reported also for another nanostructured metal oxide as ZnO nanowires [25]. When switching between different pressure conditions (ambient, scroll pump vacuum, turbomolecular pump vacuum), the samples were left to equilibrate to the new ambient conditions for at least 24 hours before measuring, as a consequence for the very long adsorption/desorption kinetics of water. Without this precaution, subsequent measurements presented reproducibility issues. The fluctuation of laboratory air humidity (about 35%) at the time of each chamber re-filling by ambient air did not influence the results as verified by means of cycled repetition of measurements.

3.1. Nature of electrical contacts

As described in the experimental section, in stack configuration, graphite (silver) paste contacts were painted onto the samples. Then, the samples can be described as a stack of TCO/ TiO_2 /graphite (silver).

The morphology of the painted and bottom contacts has been studied by SEM directly on the samples and on detached (by adhesive tape stripping) titania film fragments respectively: the roughness of the bottom surface (in contact with FTO) is found to be lower than the top surface as can be seen in figure 2 . This has also been confirmed by surface profiling of bare FTO and TiO_2 (see figure 3). Additionally the interface between FTO and nc-TiO_2 is expected to be smooth and uniform, due to the size of TiO_2 nanocrystals, while graphite paste is composed by huge flat flakes and the interface is likely to be rough. So, even though the two contact materials can be considered as metallic, the morphological difference may play a certain role.

Given these general considerations, what is really important is the nature of the two junctions (FTO/TiO_2 and graphite/TiO_2) from the energetic point of view. Our hypothesis is that under the reported experimental conditions, the contacts are ohmic - no depletion of TiO_2 occurs, on both sides. Electrical characterization in dry conditions (see figure 5-e and 5-f) supports this consideration because of the symmetric, non-rectifying behavior within the whole voltage range for stack configuration samples.

Some authors propose different interpretation about the nature of these contacts. For example O'Hayre et al. [15], working on similar unfilled mesoporous TiO_2 films, conclude that the FTO/TiO_2 is ohmic while the graphite/TiO_2 is rectifying. Snaith et al. [26], working on DSSC, conversely support the hypothesis that the Schottky barrier is present at FTO/TiO_2 contact. Anyway both groups worked on samples provided of a compact TiO_2 "blocking" layer (200 nm) to avoid shorting with respectively the top contact and the electrolyte. The electronic properties of spray-pirolysis compact layers

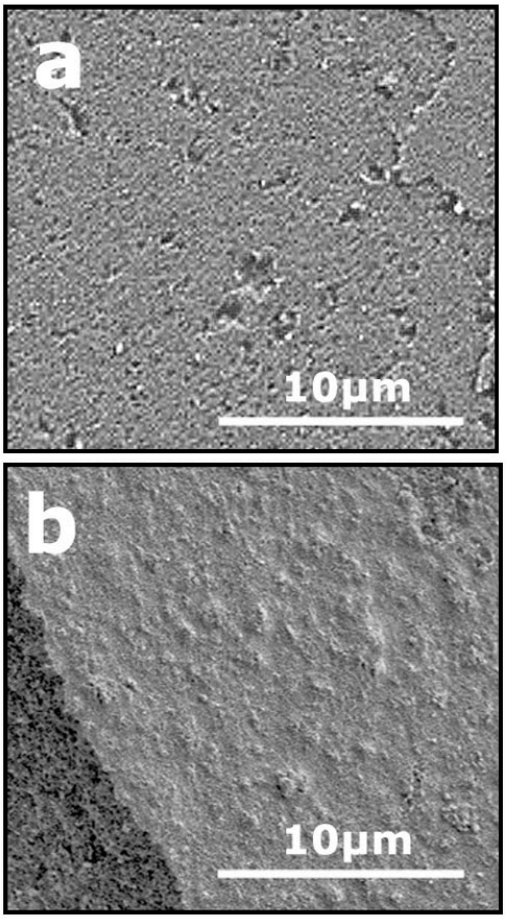

Figure 2. SEM micrographs of (a) bottom and (b) top surfaces of titania films (Dyesol)

are dramatically dependent on deposition parameters (reduction degree) and can be very different compared to the nanopowders.

We propose a flatband model consistent with these observation based on reported values [27, 28] in (figure 4). Turrion et al. [29] reported how the general picture of degenerately doped FTO may be too optimistic. Even though $SnO_2{:}F$ has a donor concentration $N_d = 10^{21}\,\mathrm{cm}^{-3}$, in presence of a percolated electrolyte the FTO may get depleted. The reported situation is certainly far from the present one. Anyway their model presents an ohmic band bending at the TiO_2 junction. So even in case of a non-metallic behavior of FTO at TiO_2 junction, our model would be still reasonable. As already pointed out, some tests with different top electrode materials, have been performed in stack configuration samples. Ag work function is 4.35 eV [30, 31], while it is 4.6 eV in the case of graphite [32, 33]. Ag and graphite as top electrode materials gave analogue results both in air and vacuum, with symmetric and resistive behavior in dry conditions. This is reasonable because in both cases the work function assumed for nc-TiO_2, 5.15 eV , is larger than the graphite and silver ones. To achieve a Schottky

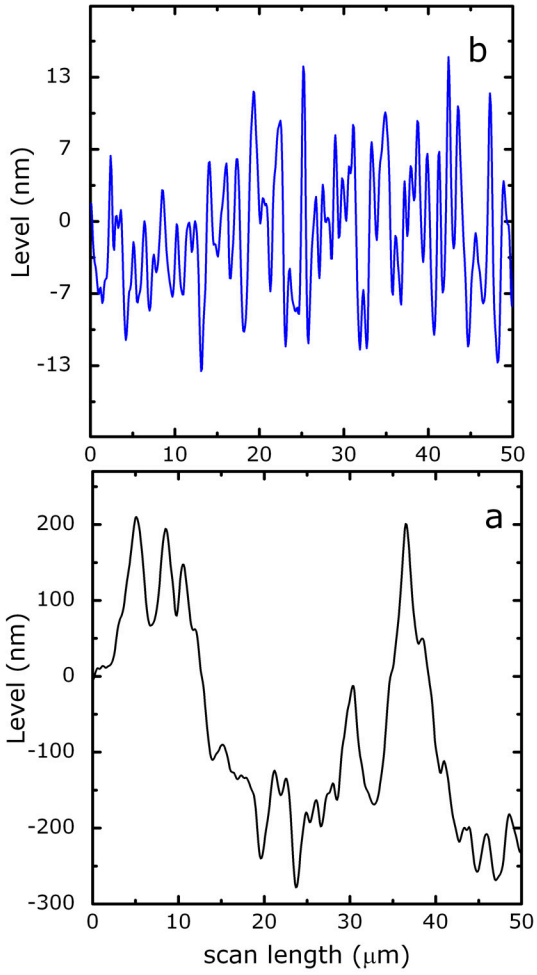

Figure 3. Surface profiles of (a) FTO surface of Dyesol sample and (b) TiO_2 top surface.

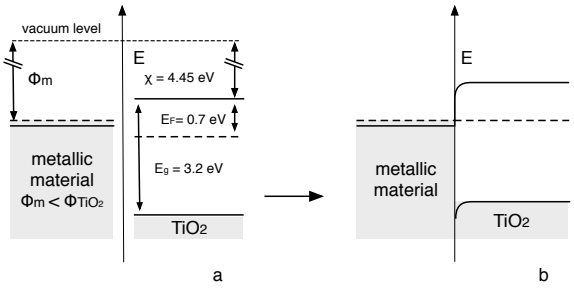

Figure 4. Energy band scheme for the present situation. In all the cases (FTO, graphite or silver contacts) the assumed Fermi level of TiO_2 lays lower than the contact material one ($\Phi_{FTO} = 4.85\,\text{eV}$, $\Phi_{grap} = 4.60\,\text{eV}$, $\Phi_{Ag} = 4.35\,\text{eV}$ w.r.t. vacuum energy level).

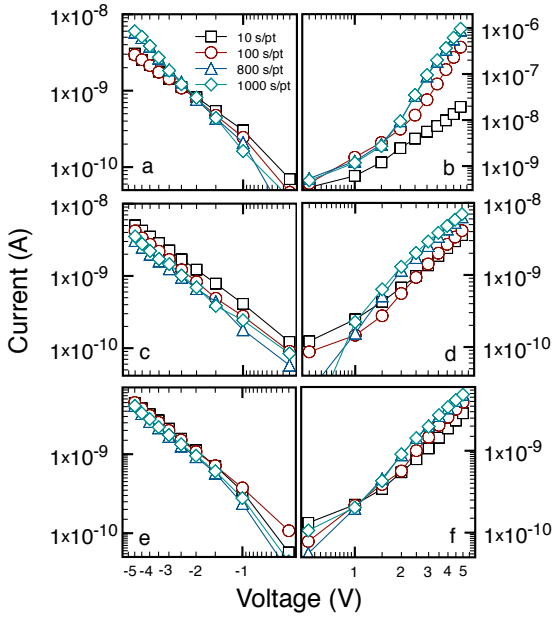

Figure 5. I-V plots of stack configuration sample. In air (a,b), low vacuum (c,d) in high vacuum (e,f). Different simbols corresponds respectively to settling time of 10, 100, 800, 1000 seconds per acquired point.

like junction, a metal with a larger work function, like Au would be necessary [34, 13].

3.2. Current-Voltage characteristics

Plots in figure 5 report current-voltage characteristics (I-V) for "standard" commercial films in stack configuration. The measurements in direct and reverse polarizations were preformed separately, always from low to high voltage values, to ensure the same measurement history for each sample. The first information that can be extracted is about the response of the system to bias voltage for different surface conditions. When comparing figures 5-b to 5-d, it appears clear that we are dealing with different transport processes expecially in air. Conversely, only a weak dependence of the I-V curves on the vacuum level is observed, compare figures 5-c and 5-e or 5-d and 5-f.

Moreover, when looking at different settling times, this fact clearly emerges (see empty squares data in figure 5-b). At a settling time of at least 100 seconds is necessary to yield a meaningful I-V characteristics and to distinguish between the behaviours in ambient air and in dry conditions. We attribute these features to the physisorbed water on the naturally hydroxylated TiO_2 surface. In fact, at RT and $P = 3.5 \times 10^{-5}$ mbar, desorption of hydroxyl groups from the TiO_2 surface is excluded, while it is expected to happen for the majority of the condensed and physisorbed water within the porous matrix. This suggests the existence of a preferential transport path on the titania surface which prevents the observation of the intrinsic material properties for samples in ambient air. In particular the immobile monolayer of physisorbed water on the hydroxylated surface, allows electron tunneling between water donor states and provides

a preferential hopping path to injected carriers [35, 36, 37].

Note that this charge carrier hopping does not occur through the intrinsic localized states distribution of TiO_2 due to its defective and oxygen deficient nature, or induced by adsorbates, but indeed through the adsorbed species. This enhanced conductivity in presence of water, is also favoured by shunting of grain-grain barriers (the main contributors to series resistance) by carriers hopping through adsorbed water donor states. As a side consideration, the electron scavenging action of adsorbed ambient oxygen on TiO_2, can be elucidated by measurements in dry air [38]. As verified by filling the chamber with dry air after sample dehydration, i.e. in minimal presence of adsorbed water but in presence of adsorbed oxygen, the conductivity is even lower than in vacuum, the opposite situation with respect to humid air.

Once the chamber is evacuated of ambient air and the sample is dehydrated, in primary vacuum conditions (figure 5-c and 5-d), the injected charge flows through another transport path, related to more intrinsic titania properties. Several works report that surface hydroxyls groups in absence of adsorbed water introduce deep electron trap states within the bandgap (1.2-1.6 eV from conduction band minimum, CBM) than the shallow ones introduced by O_2 vacancies ($<$1 eV from CBM) [39, 40, 41], and far from the Fermi level, reported to be 0.7 eV below CBM in reduced nc-TiO_2 [28]. In this picture the OH-induced localized states are deep states below to Fermi level, and in first approximation do not contribute to charge transport. So surface hydroxyls, even though present on the surface, do not dramatically affect the trasport mechanism if compared to V_O-induced Ti^{3+} centers, and our measurements can be considered to probe only the latter ones.

These have been theoretically predicted and experimentally reported by many authors as shallow levels, affecting in a dramatic way charge transport by providing additional states with fast trapping de-trapping kinetics [41, 42, 43, 44, 45, 46]. The asymmetric nature of the contacts is also evident when looking at the figure 5-a and 5-b. So presence of the surface enhanced transport path mentioned above, the limiting factor becomes carrier injection, while, in vacuum, the insulating nature of the porous metal oxide plays as a bottleneck and hides the effect of contact asymmetry. Tests with top contacts of different sizes supported the hypothesis that the nature of contacts is relevant only in presence of shunt current due to adsorbates. In vacuum the current scales correctly (linearly) with the geometric area top contact and the I-V characteristics remain symmetric and ohmic.

In order to definitely point out the importance of the adopted measurement protocol, the trends of the current flowing through the samples at a bias of 5 V in both polarizations are summarized as a function of settling time in figure 6. Even in vacuum (figure 6-b and 6-c), i.e. in dry conditions, the drift with time in the I-V is still present and influence in some way the shape of the curve, as it is common for disordered media characterized by long relaxation times [47]. The magnitude of such drift is hovewer fair, if compared with the one reported in figure 6-a, and the measurements can be considered unaffected by external contributions due to adsorbates.

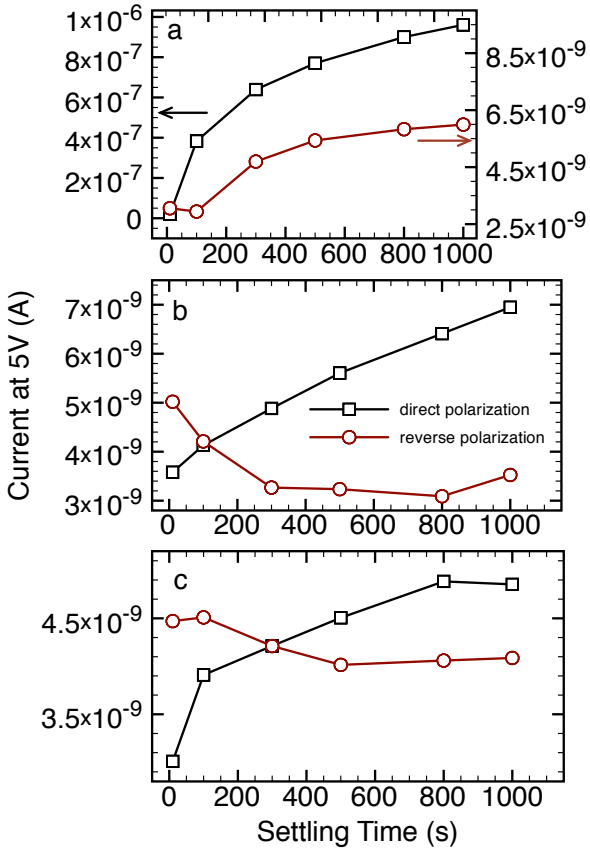

Figure 6. Current at 5 V bias as a function of measurement settling time. Air (a), low vacuum (b), high vacuum (c).

We must stress that the simple fact of leaving the samples in vacuum for 24 hours (or more) does not mean that all the physisorbed water would desorb. Moreover at the vacuum level that can be reached by our set up 3.5×10^{-5} mbar background water in the chamber is still present. Even after a degasing treatement at temperatures higher than RT (up to 380 K) the response did not change at a consistent extent. So in that range the surface could be considered in stable conditions. A way to obtain a better drying of the oxide surface could have been annealing the samples at higher temperatures. As reported in figure 7 a thermal treatment at higher temperatures, 450K for 1h in vacuum in this case, led to a dramatic change in material properties. In particular annealed sample Raman spectrum (b) features a large phototuminescence band centered around 1750 cm^{-1} that is not present in the untreated one. In the figure inset are reported the current-voltage characteristics for the same samples. Oxygen deficiency is the primary cause of n-type behavior of TiO_2 and we assign the larger conductance of heated sample (b) to a larger concentration of oxygen vacancies due to annealing. Moreover oxygen vacancies cause photoluminescence in nanocrystalline anatase [48] which is confirmed by Raman spectra. Linear fits on double logartithmic scale for the data reported in figure 7-inset serve as a check for the ohmic behavior at low voltages. The fitted slopes

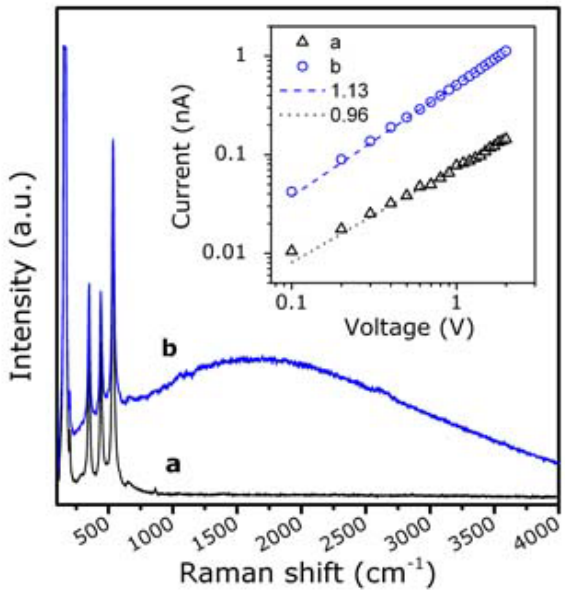

Figure 7. Main plot shows Raman spectra of (a) untreated and (b) vacuum annealed (3.5×10^{-5} mbar, 450K for 1h) titania film (Dyesol). In the inset are reported the low voltage characteristics in vacuum, before and after the annealing, for the same sample.

are respectively 0.960 ± 0.018 and 1.130 ± 0.005 for the untreated and annealed samples. So the regime is not perfectly ohmic, but given the complex nature of the interfaces, and the huge deviations in slopes at the SCL regime onset at higher voltages, it is reasonable to consider this as the ohmic regime.

It can be now stressed how a suitable measurement procedure reveals the limits set by this sample configuration. The electrical characterization of samples with working electrodes in sandwich configuration, is in fact limited by some issues. The high resistivity of titania [16, 14] implies very large series resistance for 15 µm thick nanoporous samples in stack configuration. Hence very large voltage values are mandatory to achieve high injection rates, in order to rise the Fermi level and influence the contribution to transport of the band gap states. In fact in dehydrated stacked samples, no onset of SCL regime is observed, even up to 15 V bias voltage. On the other hand thin samples (less than 1 µm) are exposed to short circuit issues unless a blocking compact TiO_2 layer is present. Such a blocking layer would introduce an additional complexity due to the presence of new interface structures between FTO and nc-TiO_2.

We observed instead some deviation toward SCL behavior in the planar sample configuration (see figure 8). This means the injected carrier concentration is now high enough to reach a trap filling regime also in vacuum. The transition from a slope of 1 to a slope of more than than 2 is the signature of an exponential trap distribution [22, 23, 49]. Note that in air, the effect of adsorbed species is still observable, consistently with former samples even though the effect is reduced because of the smaller probed volume (compare empty triangles in figure 8 and figure 1-b).

In summary the presence of adsorbates on mesoporous TiO_2 yields a band gap

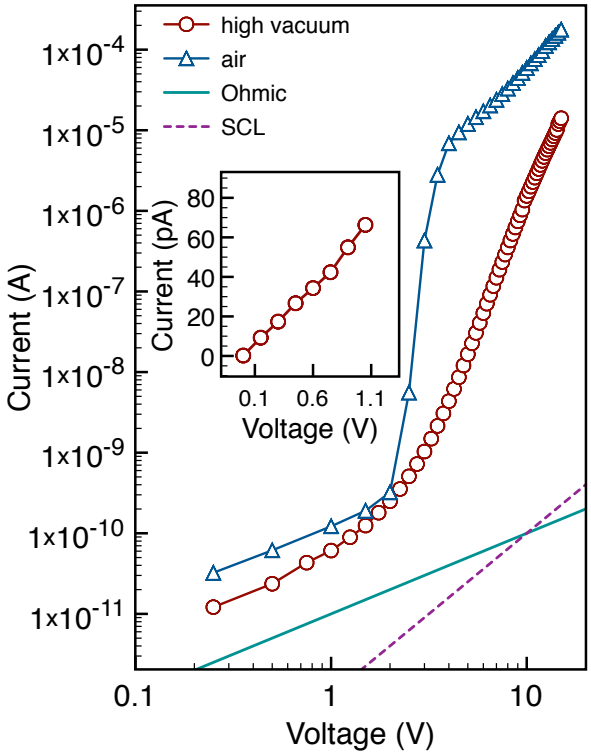

Figure 8. I-V characteristics of planar configuration sample. In air (trinagles) and vacuum (circles, P = 3.5×10^{-5} mbar). Linear (solid line) and square (dashed line) slopes are also reported as a guide. The inset reports the detail of low voltage ohmic regime in vacuum. This measurement configuration allows for resolving BGS features in both wet and dry conditions. All curves are related to 1000 s/pt measurements.

states signature compatible with the ones obtained on filled DSSC (exponential traps distribution) but it is not an intrinsic property of the semiconductor, while, in dry conditions, even though the titania surface is not absolutely "clean", the BGS signature is still compatible with an exponential BGS distribution, but with different properties. This means that by this measurement technique proper quantitative result about TiO_2 electronic properties could be obtained (trap concentration, effective mobility).

Although hydroxylated titania is not a completely intrinsic system, and avoiding thermal treatments could limit the dehydration of the surface, by the application of a suitable measurement protocol and sample configuration, the obtained results are surely more related to its intrinsic properties rather the ones obtained in more complex systems.

Different samples of the same commercial stock (Dyesol) confirmed the reproducibility of the results, I-V measurements on P25 based samples (same contact geometry and similar dimensions of Dyesol ones) are in total agreement with data from commercial TiO_2 films. A conclusion corroborated by SEM micrographs which confirmed analogue porous morphologies. This similarty is also consistent with the results obtained from the measurements on planar geometry samples, also P25 based,

although in this case the planar samples behaved as less sensitive to measurement history and variation of ambient conditions, an effect that can be tentatively ascribed to the smaller titania probed volumes.

4. Conclusions

Our results highlight experimental issues of primary concern when interested in electrical characterization of mesoporous nc-TiO_2, that are not always evident in literature. The choice of longer settling times allowed to explicitly discriminate residual charge transport contributions from adsorbed water. Under suitable sample surface conditions and measurement settling times we had access to a more intrinsic electrical behavior (both magnitude and shape of I-V) of the mesoporous electrodes. Our tests on a different sample configuration made possible to go beyond the ohmic regime and to get information about localized states in a regime of space charge limited current. This configuration probes a smaller volume of titania avoiding the large series resistance of typical DSSC electrodes while eliminating the problem of shorting in very thin stack samples and consequently the presence of an additional compact TiO_2 blocking layer between FTO and porous titania. It must be stressed that the present planar geometry is not the common coplanar electrode configuration but it yields volume information. The possible compromise between thermal treatment and stoichiometric stability in mesoporous titania should be deeper investigated, for this reason our measurement protocol does not include sample annealing at the moment. Finally the shape of the I-V of the planar sample geometry indicates that the localized states distribution measured on dry samples may be substantially different from the one present in the electrolyte filled porous systems. This results represent also a connection between experimental investigations of filled porous systems and theoretical studies on clean-surface TiO_2. It will also be fundamental to investigate in depth different band gap states signatures in presence of different probe adsorbates, in order to clarify the interaction between pore-filling species and TiO_2 transport properties.

References

[1] O'Regan B and Gratzel M 1991 *Nature* **353** 737–739
[2] Peter L M 2007 *Phys. Chem. Chem. Phys.* **9** 2630–2642
[3] Sberveglieri G, Comini E, Faglia G, Atashbar M and Wlodarski W 2000 *Sensor Actuat B-Chem.* **66** 139–141
[4] Mun K S, Alvarez S D, Choi W Y and Sailor M J 2010 *ACS nano* **4** 2070–2076
[5] Hoffmann M R, Martin S T, Choi W and Bahnemann D W 1995 *Chem. Rev.* **95** 69–96
[6] Usseglio S, Damin A, Scarano D, Bordiga S, Zecchina A and Lamberti C 2007 *J. Am. Chem. Soc.* **129** 2822–2828
[7] Henderson M A 2011 *Surf. Sci. Rep.* **66** 185 – 297 ISSN 0167-5729
[8] Martyanov I N and Klabunde K J 2004 *J. Catal.* **225** 408–416
[9] Ito S, Chen P, Comte P, Nazeeruddin M K and Liska P 2007 *Prog. Photovoltaics* **15** 603–612
[10] Macak J M, Tsuchiya H, Taveira L, Aldabergerova S and Schmuki P 2005 *Angew. Chem. Int. Ed.* **44** 7463–7465

[11] Bisquert J 2008 *Phys. Rev. B* **77** 203–235
[12] Gagliardi A, Gentilini D and Carlo A D 2012 *J. Phys. Chem. C* **116** 23882–23889
[13] Konenkamp R, Wahi A and Hoyer P 1994 *Thin Solid Films* **246** 1613
[14] Eppler A M, Ballard I M and Nelson J 2002 *Physica E* **14** 197
[15] O'Hayre R, Nanu M, Schoonman J and Goossens A 2007 *J. Phys. Chem. C* **111** 4809–4814
[16] Pomoni K, Vomvas A and Trapalis C 2008 *J. Non-Cryst. Solids* **354** 4448 – 4457
[17] Chen Z and Lu C 2005 *Sens. Lett.* **3** 274–295
[18] Long R, Dai Y and Huang B 2013 *J. Phys. Chem. Lett.*
[19] Long R 2013 *J. Phys. Chem. Lett.* **4** 1340–1346
[20] Oh W C, Jung A R and Ko W B 2007 *J. Ind. Eng. Chem* **13** 1208–1214
[21] Oh W and Chen M 2008 *Bulletin-Korean Chemical Society* **29** 159
[22] Rose A 1955 *Phys. Rev.* **97** 1538–1544
[23] Lampert M A 1956 *Phys. Rev.* **103** 1648–1656
[24] Cavallini A and Polenta L 2008 *in: Characterization of semiconductor heterostructures and nanostructures, (Lamberti C Ed) Elsevier, Amsterdam, p.* 55 – 91
[25] Hullavarad S, Hullavarad N, Look D and Claflin B 2009 *Nanoscale Res. Lett.* **4** 1421–1427
[26] Snaith H J and Gratzel M 2006 *Adv. Mater.* **18** 1910–1914
[27] Levy B, Liu W and Gilbert S E 1997 *J. Phys. Chem. B* **101** 1810–1816
[28] Cahen D, Hodes G, Graetzel M, Guillemoles J and Riess I 2000 *J. Phys. Chem. B* **104** 2053 – 2059
[29] Turrion M, Bisquert J and Salvador P 2003 *J. Phys. Chem. B* **107** 9397–9403
[30] Mitchell E W J and Mitchell J W 1951 *Proc. R. Soc. Lond. A.* **210** 70–84
[31] Chelvayohan M and Mee C H B 1982 *J. Phys. C: Solid State Phys.* **15** 2305
[32] Krishnan K S and Jain S C 1952 *Nature* **169** 702–703
[33] Willis R F, Feuerbacher B and Fitton B 1971 *Phys. Rev. B* **4** 2441–2452
[34] Szydlo N and Poirier R 1980 *J. Appl. Phys.* **51** 3310–3312
[35] Khanna V and Nahar R 2000 *J. Phys. D: Appl. Phys.* **19** 141–145
[36] Korotchenkov G, Brynzari V and Dmitriev S 1999 *Sensor Actuat B-Chem.* **54** 197–201
[37] Sun C, Liu L M, Selloni A, Lu G Q M and Smith S C 2010 *J. Mater. Chem.* **20** 10319–10334
[38] Livraghi S, Paganini M C, Giamello E, Selloni A, Di Valentin C and Pacchioni G 2006 *J. Am. Chem. Soc.* **128** 15666–15671
[39] Di Valentin C, Pacchioni G and Selloni A 2006 *Phys. Rev. Lett.* **97** 166803
[40] Amore Bonapasta A, Filippone F, Mattioli G and Alippi P 2009 *Catal. Today* **144** 177–182
[41] Shibuya T, Yasuoka K, Mirbt S and Sanyal B 2012 *J Phys. Condens. Mat.* **24** 435504
[42] Boschloo G and Fitzmaurice D 1999 *J. Phys. Chem. B* **103** 2228–2231
[43] Kumar P M, Badrinarayanan S and Murali S 2000 *Thin Solid Films* **358** 122–130
[44] Iijima K, Goto M, Enomoto S, Kunugita H, Ema K, Tsukamoto M, Ichikawa N and Sakama H 2008 *J. Lumin.* **128** 911–913
[45] Minato T, Sainoo Y, Kim Y, Kato H, Aika K, Kawai M, Zhao J, Petek H, Huang T, He W *et al.* 2009 *J. Chem. Phys.* **130** 124502–124513
[46] Finazzi E, Di Valentin C and Pacchioni G 2009 *J. Chem. Phys. C* **113** 3382–3385
[47] Konenkamp R 2000 *Phys. Rev. B* **61** 11057–11064
[48] Zhang W, Zhang M, Yin Z and Chen Q 2000 *Applied Physics B* **70** 261–265
[49] Bubel S, Mechau N, Hahn H and Schmechel R 2010 *J. Appl. Phys.* **108** 124502–124508